Migration Letters

Volume: 20, No: S4(2023), pp. 496-521

ISSN: 1741-8984 (Print) ISSN: 1741-8992 (Online)
www.migrationletters.com

The Effect of Impact Loading on the Various Properties of Improved Non-Reinforced Masonry Elements by Utilizing Flexible Fiber-Reinforced Concretes

Seyedmohammad Amini[1], Alireza Mirjalili[2], Mohammadreza Javaheri[3]

Abstract

The utilization of flexible fiber-reinforced concretes, including engineered cementitious composites (ECCs), to retrofit unreinforced masonry walls is crucial due to their brittle behavior and limited flexibility. In this context, it is essential to consider how well such materials perform when utilized as a reinforcement layer for unreinforced masonry walls to enhance their behavior (flexibility and strength) when subjected to dynamic stresses, notably impact loads. Through nonlinear dynamic impact analysis, the current research assesses and compares the vertical middle displacement, energy, and distribution of plastic strains in unreinforced masonry materials under two conditions, i.e., non-retrofitted and retrofitted with a one- or two-side cover of ECC layers under dynamic impact loading. The ECC reinforcing layers thickness, stiffness, and placement location of middle or sides of the top surface with full connection were changed to examine the vertical displacement, Energy dissipation and plastic strains distribution of the non-reinforced masonry specimen during the vertical impact loading. Introducing ECC layers to unreinforced masonry materials enhanced their behavior against out-of-plane impact loads, dissipated energy, and minimized plastic strains and cracks.

Keywords: *ECC, non-reinforced masonry wall, impact loading, FEM.*

1. Introduction

There are numerous unreinforced masonry (URM) structures worldwide (Niasar, Alaee, & Zamani, 2020). Earthquakes have shown the poor seismic performance of traditional URM buildings (Riahi, Elwood, & Alcocer, 2009). URM buildings have a large degree of seismic vulnerability on account of ineffective design and construction and low material quality (Niasar et al., 2020). Earthquakes could damage such structures around the world (Engineers, 2017; Maghfouri, Shafigh, Alimohammadi, Doroudi, & Aslam, 2020). An in-plane shear load can damage URM buildings, in which case the out-of-plane performance of infill/bearing URM walls is of great importance as it could threaten structural stability (Kumar & Rai, 2022; Leblouba et al., 2022). Hence, apart from the investigation of pre-earthquake URM building retrofitting, post-earthquake retrofit approaches are to be examined (Dizhur et al., 2011).

A large number of retrofit approaches have been developed and experimentally verified for URM buildings in recent decades (Deng & Yang, 2020). Reinforced-concrete (CR) coatings and welded wire meshes and mortars are among traditional retrofitting techniques, in which a 50-100mm thick cement mortar layer or steel mesh is applied to

[1] Ph.D student, Department of civil engineering, Taft branch, Islamic Azad University, Taft, Iran
[2] Assistant professor, Department of civil engineering, Yazd branch, Islamic Azad University, Yazd, Iran
[3] Assistant professor, Department of civil engineering, Yazd branch, Islamic Azad University, Yazd, Iran

masonry walls (Ghiassi, Soltani, & Tasnimi, 2012; Kadam, Singh, & Li, 2014). Polymers have been recently employed as a new retrofit approach. Fiber-reinforced polymer (FPR) retrofitting is employed to enhance ductility and strength in masonry walls used for in-plane load bearing (Luccioni & Rougier, 2011; Maghfouri et al., 2022; Nezhad, Kabir, & Banazadeh, 2016). However, Research has shown that FPR sheet debonding would be the dominant failure mechanism in retrofitted masonry walls. Furthermore, The drawbacks of FRP-retrofitted infill masonry walls include epoxy expensiveness, surface preparing, and epoxy-wall inconsistency. To handle such drawbacks, researchers have employed cementitious composites to enhance seismic behavior in light of increased compatibility, affordability, availability, constructability, easy implementation, and unique physico mechanical properties, e.g., negligible post-retrofit shrinkage and satisfactorily low thermal expansion (Alimohammadi et al., 2021; Sharbatdar & Tajari, 2021). Polymer meshes and cementitious mortars have also been exploited for masonry wall retrofit. The polymer and mortar retrofit techniques include textile-reinforced concrete (TRC), textile-reinforced mortar (TRM), inorganic Matrix-Grid (IMG) or cementitious MatrixGrid (CMG), engineered cementitious composite (ECC), and fabric-reinforced cementitious matrix (FRCM) (Bernat-Maso, Escrig, Aranha, & Gil, 2014; Carozzi, Milani, & Poggi, 2014; Ismail, El-Maaddawy, & Khattak, 2018; Yardim & Lalaj, 2016).

It should be noted that ECC is a member of the fiber-reinforced concrete (FRC) family (Han, Feenstra, & Billington, 2003). It shows pseudo-strain-hardening behavior due to tensile multiple cracking (Li & Leung, 1992; Pan, Wu, Liu, Wang, & Liu, 2015). It also undergoes multiple shearing cracking. The Ohno shear and Iosipescu shear tests can be used to demonstrate multiple shearing cracking (Li et al., 1994) (van Zijl, 2007). Researchers have therefore described ECC as a material of external bonding to retrofit masonry structural components (Dehghani, Nateghi-Alahi, & Fischer, 2015; Deng & Yang, 2018).

ECC-retrofitted masonry components have been reported to experience substantial improvements in shear resistance, ductility, and lateral stiffness. Many numerical works demonstrated the performance enhancement of ECC-retrofitted masonry components (Deng & Yang, 2020). ECC has shown self-controlled crack width under incremental loads, in contrast to high-performance FRC (Renuka & Mervin Sanjith, 2022). In general, ECC has been reported to play a key role in the behavior improvement of structures. IT has been a promising candidate in seismic retrofit in light of handling URM structure shortcomings, e.g., brittleness, softening, and poor tensile strength (Zamani Ahari & Yamaguchi, 2021).

Deng and Yang (Deng & Yang, 2018) studied ECC-retrofitted URM walls. They tested a total of six half-scale ECC-retrofitted and non-retrofitted masonry walls under static cyclic lateral loads. They retrofitted two walls with strip-pattern ECC mortar and completely retrofitted two other masonry walls using an ECC mortar of a fixed thickness. The retrofit approaches were found to be effective and efficient in enhancing URM walls in ductility and lateral strength. ECC-retrofitted masonry walls have shown different failure mechanisms in different ECC patterns. Strip-coated masonry walls showed diagonal failure, while fully coated walls underwent rocking failure – the failure mode of non-retrofitted walls was diagonal. It was found that loading conditions, wall parameters, retrofit conditions, and ECC mortar pattern had significant effects on the lateral strength, energy absorption, and failure mechanism of URM walls. Santa-Maria et al. (Santa-Maria & Alcaino, 2011) and Konthesingha et al. (Konthesingha et al., 2013) analyzed the post-damage behavior of external FRP-retrofitted masonry walls. They reported similar URM wall performance enhancements, regardless of the pre-retrofit damage extent.

Soleimani-Dashtaki et al. (Soleimani-Dashtaki, Ventura, & Banthia, 2017) subjected sprayable eco-friendly ECC-retrofitted URM walls to shaking table testing in order to measure the lateral bearing capacities of single- and double-face retrofitted walls. It was found that the single-face retrofit was efficient for low-rise buildings under major seismic

loads, while high-rise structures required double-face retrofitting to resist large wall loads. Zhang et al. (Zhang, Maalej, & Quek, 2004) implemented optimal low- and high-modulus fiber volume ratios to introduce a hybrid-fiber ECC (HF-ECC) in order to more effectively meet functional requirements in buildings resistant to blast and impact loads. Singh et al. (Singh, Patil, & Munjal, 2017) evaluated a sandwich-like ECC-retrofitted epoxy-coupled beam in out-of-plane behavior. They reported that prefabricated ECC enhanced masonry beams in deformability and stiffness (Tabrizikahou, Kuczma, Łasecka-Plura, & Noroozinejad Farsangi, 2022). A review of the literature suggests that the use of ECC on the two faces of a URM masonry wall could enhance its ductility (Deng, Dong, & Ma, 2019).

The present work sought to experimentally evaluate ECC-retrofitted masonry walls under out-of-plane impact and quasi-static loads. Bearing walls are a major element of masonry structures and are responsible for resisting lateral and gravitational loads. These elements, however, could result in localized and progressive failure and collapse in a masonry building due to poor strength. It is necessary to evaluate and retrofit such walls, specifically under dynamic loading (such as impact loading). The concrete lining could improve both out-of-plane behavior and in-plane performance in bearing walls. The contributions of ECC to the performance of brick walls have not been explored in Iran. The novelty of this paper lies in the particular properties of Iranian bricks and mortars.

2. Materials and method

2.1. Methodology

In general, the finite element method (FEM) is used to simulate and evaluate the dynamic behavior of structural components. In recent decades, FEM has been increasingly applied in the micro- and macro-modeling and dynamic analysis of complex engineering issues, including structural components, since it is the most prevalent approach in continuous settings. FEM uses explicit (time-dependent) or implicit formulations. ABAQUS is one of the most effective FEM software packs supporting explicit and implicit formulations. It can employ two-dimensional, and three-dimensional elements in continuous settings and conduct micro- and macro-simulations of structural components (such as masonry walls) and fiber-reinforced concretes. FEM enables modeling ECC-retrofitted URM walls and assessing their dynamic impact behavior. Consequently, ABAQUS micro-scale three-dimensional simulations were used in the current investigation, where:

- A homogeneous mass relying on the elastoplastic behavior model, which models the similar blocks of the masonry units and the surrounding mortar utilizing a hybrid plastic-failure model to characterize plastic masonry behavior,

- To simulate the connection of the similar blocks, contact elements with an appropriate behavior model are used,

- Homogeneous mass relying on the elastoplastic behavior model, where a hybrid plastic-failure model defines the plastic behavior of the ECC layers,

- To stabilize the numerical models, appropriate boundary conditions are given to the specimens, and

- Under impact loading, the nonlinear dynamic analysis of the specimens is accomplished while assessing the specimens' out-of-plane behavior (i.e., ductility and strength) under the load.

2.2. Assessment and validation of the study's numerical simulation findings for the laboratory sample

Now, according to Fig. 1, the lateral load-bearing capacity of the laboratory sample during the analysis is assessed by the nonlinear static method under uniform lateral

loading to guarantee the precision of numerical simulations and the software employed for this objective (Abaqus software) in the research. Afterward, according to Table S1, it corresponds with the load-bearing measured during the experiment.

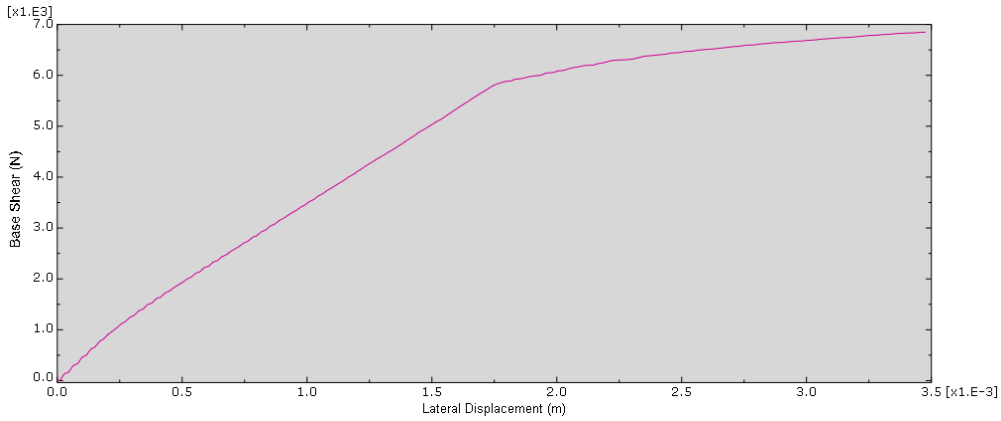

Fig. 1. Lateral load-bearing curve - lateral deflection of the laboratory sample during numerical analysis

When the predefined uniform lateral deflection is applied to the laboratory sample step by step during the nonlinear static analysis of the sample, excellent agreement (with a maximum tolerance of about 6.3%) between the lateral load-bearing calculated during the experiment and the load-bearing measured from the experiment is shown in Fig. S3 and Table S1. This demonstrates confidence in the accuracy of the numerical simulations and the software employed in the investigation (Abaqus).

2.3. Experimental works using experimental specimens

It is necessary to assess the ECC thickness, the ECC number of layers, and the ECC type to examine the behavior of ECC-retrofitted unreinforced masonry (URM) buildings under impact loads. Therefore, for each parameter, at least two factors should be taken into account. For every component, a minimum of three specimens should be created. The combined impacts of such characteristics also require to be researched.

There were 18 specimens created. Six specimens were built to investigate the impact of ECC layer location (top and/or top and bottom layers). Six specimens were used to determine the location of the ECC layer (totally contentious or discontinuous in the middle of the specimen). In addition, three specimens were utilized as controls, whereas the remaining three were employed to investigate the combined impact of the parameters.

The impact test was conducted on the experimental specimens once they had been fabricated using the necessary parameters. Specific cameras were used to capture the impact process, and software was used to evaluate the specimens' impact loads. Micro-scale and three-dimensional simulations of ECC-retrofitted and non-retrofitted URM specimens were performed based on the given geometric and mechanical characteristics. On the specimens, the boundary conditions and meshing were applied. The subjects were subsequently exposed to impact loads. The specimens' out-of-plane behavior (ductility and strength) under the loads was evaluated using a nonlinear dynamic analysis of the specimens under the loads.

2.4. Non-reinforced masonry modeling

Ten isotropic and homogeneous masses are utilized for micro numerical modeling of bricks in the non-reinforced masonry sample:

1. In the form of comparable blocks (including a masonry unit and its adjacent mortar) as illustrated in Fig. S1.

2. with a design based on Fig. S1

3. Measuring 210, 75, and 102 mm in length, width, and height

4. By using a plastic-damage combination model to define the plastic behavior with an elastoplastic behavior

In 3D simulations, unreinforced masonry has been modeled using a simpler microtechnique. As part of this technique, masonry is represented utilizing equivalent blocks, including masonry units and their mortar proximity. Equivalent blocks (75 mm wide) will be joined by adequate connections, consisting of brick (65 mm wide) and half of its adjacent mortar (10 mm thick). Therefore, numerical modeling of the interaction between adjacent bricks is needed to determine the behavior caused by the mortar (existing in joints between bricks) in the non-reinforced masonry sample. The friction coefficient (surface roughness), which is crucial for defining the shear behavior of the components, is employed at the interface of adjacent bricks when contact elements with shear and normal behavior are employed.

Importantly, the equivalent models' respective specific weights, elasticity modulus, Poisson's ratio, compressive, tensile, and dilation strengths seem to be 18.5 KN/m3, 3500 Mpa, 60 Mpa, 6 Mpa, and 10 degrees. The plastic behavior and qualities of equivalent models will be specified in addition to their physical and elastic properties. To address the damage standard of the brick (using its two primary failure modes, tensile cracking and compressive crushing), a combined plastic-damage model was utilized for bricks. This model is indeed a continuous plastic model.

1. Brick's strain-stress curve under uniaxial compressive force

2. Brick's strain-stress curve under uniaxial tensile force

A correlation between the brick's compressive strain and stress is necessary for determining the strain-stress curve under uniaxial force. The simulation employs the following equation to accomplish this objective (Kent and Park, 1971):

$$\sigma_c=f'_c\ [2(\varepsilon_c/\varepsilon'_c\ )-(\varepsilon_c/(\varepsilon'_c)^2] \qquad (1)$$

Where σc and εc are compressive strain and stress, respectively, f'c and ε'c are the brick's compressive strength (in this simulation 60Mpa) and its associated strain (0.0024 in our simulation due to Park and Paula, 1975). The equation develops a curve in which the behavior of the brick is linear until it reaches its compressive strength. It continues after achieving 20 percent of this strength since the brick retains 20 percent of its compressive strength under significant compressive strains. Consequently, based on the curve and the equation, compressive plastic strains are computed for compressive strength and employed to describe the compressive plastic behavior of the equivalent blocks. The brick's strain-stress curve is described in the following sections regarding the brick's tensile strength (6 Mpa in this simulation) and linear elastic behavior up to that point (strain-stress curve peak under uniaxial tension).

2.5. Modeling of ECC layers in the non-reinforced masonry sample

Homogeneous masses are employed for the numerical modeling of ECC layers in the unreinforced masonry sample:

1. Along with specified thickness (t)

2. On the bottom or top surfaces of the sample, entirely or partially

3. With or without a complete connection to the sample's top or bottom surfaces

4. An elastoplastic behavior model that defines the plastic behavior utilizing a combined plastic damage model

Considering that the interfaces between the sample and the layers are fixed, the tie constraint is utilized to numerically simulate a full connection for ECC layers to the non-reinforced masonry sample. Contact elements (with normal and shear behavior) at such

interfaces describe numerical modeling of the incomplete connection between the ECC layers and the non-reinforced masonry sample. When describing the shear behavior of these components, the coefficient factor (surface roughness) must be taken into account. The plastic behavior and qualities of ECC layers will be described in addition to their physical and elastic features. For ECC layers, a combined plastic-damage model is applied. As noted previously, the model uses two primary failure processes, particularly tensile cracking, and compressive crushing, to analyze the damage criteria of materials. Firstly, Table 1 (acquired from the compressive test on the ECC) is used to develop the compressive strain-stress curve of ECC layers.

Table 1. Values of the stress-strain of stress curve of ECC layers (Rezaei, Hamidi, & Farshi Homayoun Rooz, 2016)

Yield Stress (MPa)	**Inelastic Strain × 10 $^{-3}$**
19.62	0.00
28.08	2.80
36.79	5.70
49.60	9.90
56.89	12.70
62.78	17.00

Tensile stress-strain curve values for ECC layers will be determined in the paragraphs that follow the following Table 2 (acquired from the tensile test on ECC).

Table 2. Values of the stress-strain of tension curve of ECC layers (Rezaei et al., 2016)

Yield Stress (MPa)	**Inelastic Strain × 10 $^{-3}$**
1.45	0.00
1.06	5.70
0.43	13.80

2.6. Boundary conditions modeling

2.6.1. Models meshing

Masses in models are meshed utilizing continuous 3D 8-node components (referred to as C3D8 in the Abaqus software). (Figs. S3-6).

3. Results and discussion

The vertical displacement, energy, and intensity of the plastic strains of a non-reinforced masonry material sample under two different conditions—retrofitting and non-retrofitting with the one-sided coating (in two positions—on the sample's above and below the surface) and double-sided coating of ECC layers throughout vertical impact loading (during nonlinear dynamic analysis) of the sample's middle—are analyzed in the current section. Furthermore, the influence of ECC reinforcement layers on the out-of-plane dynamic loading behavior of unreinforced building material walls is investigated, as is the role of double-sided coating (especially in comparison to one-sided coating) and the position of ECC reinforced layers (on the top or bottom of the sample). Altering the location of ECC-reinforced layers in the two-sided coating - where it is supposed to be in the middle or on the top and bottom surfaces of the sample - modifying the connection of the bottom surface of the sample with the ECC-reinforced layer in the one-sided coating, altering the thickness (from 7.5 to 30 mm) and modulus of elasticity (from 15 to 22.5 GPa) of ECC-reinforced layers in the two-sided coating. The effect dynamic behavior of off-plane walls of unreinforced building materials is investigated to determine the role of location (in the middle or on the sides of the above and bottom surfaces of the sample) reinforced with ECC layers, type of connection (detachment or complete connection) of

ECC reinforced layers with building materials and the hardness and thickness of ECC reinforcement layers.

3.1. Evaluating the obtained results from numerical simulations

Importantly, the decreased percentages of the vertical displacement in the center (ΔU/U0), energy (ΔE/E0), and plastic strain (Δε/ε0) of the specimen were also analyzed in every mode depending on the values of the dimensionless parameters. U0, E0, and ε0 are the maximum vertical displacement in the center, the energy, and the plastic strain of non-retrofitted unreinforced masonry materials. Consequently, ΔU, ΔE, and Δε represent the difference in the values of the relevant parameters under two scenarios, namely non-retrofitted and retrofitted with ECC layers.

According to Figs. 2 (a,b), by reinforcing the non-reinforced masonry sample with ECC layers (especially with a two-sided cover on the whole top and bottom surfaces), the vertical impact displacement of the middle of the specimen is considerably reduced. Furthermore, we observe that the reinforcement of the non-reinforced masonry sample with one ECC layer on the whole bottom surface of the specimen and two ECC layers in the middle of the top surface of the sample (in comparison to an ECC layer on the whole bottom surface and one ECC layer on sides of the top surface of the sample) led to a more pronounced (and closer to the two-sided cover in the whole bottom and top surface of the specimen) function in increasing the out of plane strength and reducing the vertical displacement in the middle of this specimen during the impact loading. Thus, in reinforcing the non-reinforced masonry with one ECC layer on the whole bottom surface and one ECC layer on the sides of the top surface of the sample, ECC layers show a poorer (and closer to the one-sided cover on the whole bottom surface of the specimen) performance in increasing the out of plane strength and finally, reduction of the vertical displacement in the middle of the specimen during the impact loading.

Therefore, the figures indicate a proper function from ECC reinforcing layers (especially in the whole bottom and middle of the top surface of the specimen) in reducing the non-reinforced masonry deformation during the impact loading and ultimately improvement of the out-of-plane impact dynamic behavior of this specimen. This function becomes more reliable by the two-sided covering of this specimen using ECC reinforcing layers (compared to a one-sided cover on the whole specimen's bottom surface and also covering the whole bottom surface and sides of the top surface of the specimen).

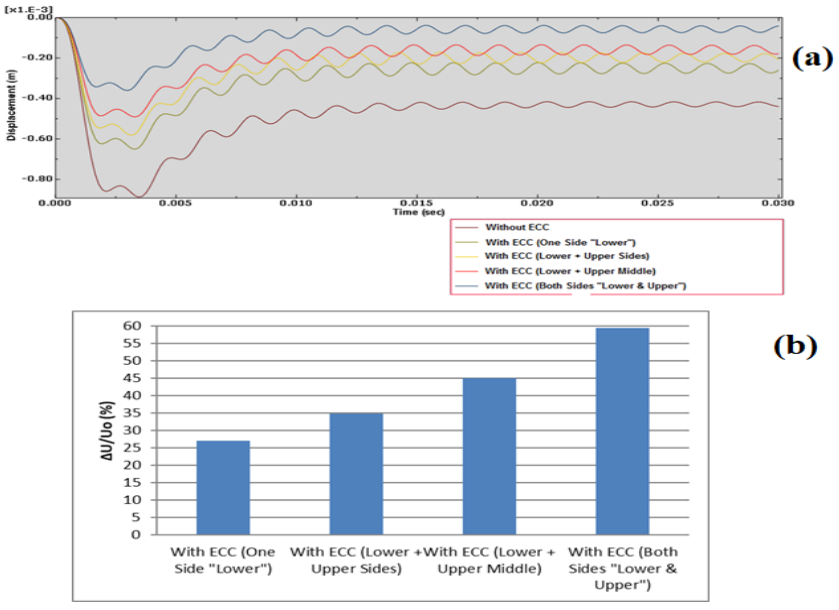

Fig. 2. The effect of the ECC reinforcing layer and the placement location of the top layer (middle or perimeters of the top layer with a full connection) on the a) vertical

displacement and b) reduction percentage of vertical displacement of the middle of non-reinforced masonry in two-sided covers during impact loading (t=15 mm، E_ecc=17.5 GPA)

Moreover, according to Fig. 3 (a,b), ECC layers provide a more significant performance (and closer to the two-sided cover performance on the whole bottom and top surface of the sample) in energy absorption and dissipation (energy reduction) of this specimen during the impact loading. Additionally, reinforcement of non-reinforced masonry specimens with an ECC layer on the whole bottom surface and an ECC layer on the top surface resulted in lower performance (and more comparable to the performance of the one-sided cover on the entire bottom surface of the sample) in absorption and dissipation of energy (energy reduction) of this specimen during the impact loading. Therefore, the above figures generally show the appropriate function of the ECC reinforcing layers (especially on the entire bottom and middle of the top surface of the specimen) in energy dissipation (energy reduction) of the non-reinforced masonry specimen during the impact loading and ultimately improvement of the out of plane impact dynamic behavior of it. This proper function becomes more suitable by the two-sided covering of this sample using ECC reinforcing layers (compared to one-sided covering on the entire bottom surface of the sample and covering the entire bottom surface and sides of the top surface of the specimen).

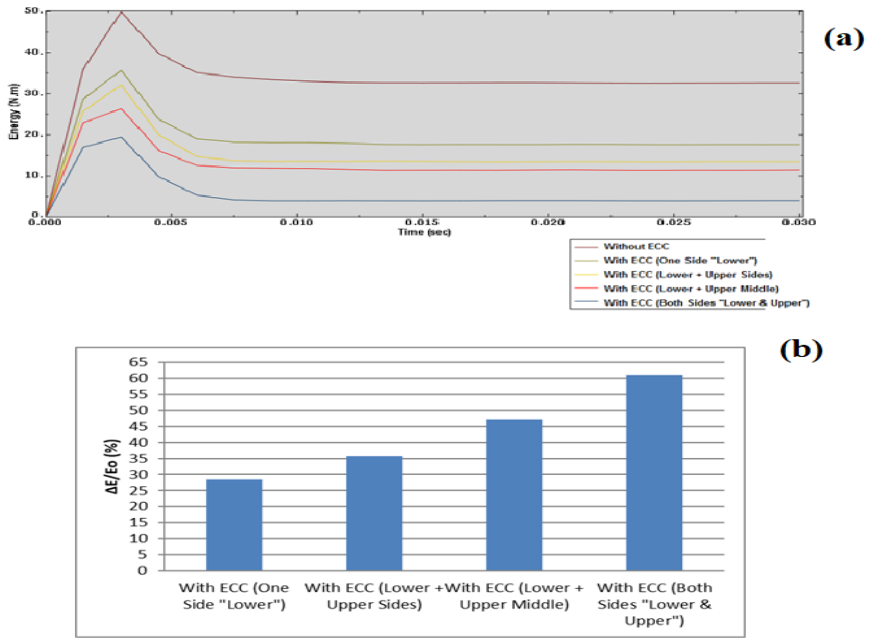

Fig. 3. Effect of ECC reinforcing layers and top layer placement location (middle or sides of the top surface with full connection) on the a) energy and b) on the reduction percentage of the non-reinforced masonry energy during vertical impact loading in two-sided covering (t=15 mm، E_ecc=17.5 GPA)

According to figs. S7 and S8, when the non-reinforced masonry specimen is strengthened with ECC layers (especially with a two-sided cover on the entire bottom and top surfaces) during impact loading, the distribution and concentration of plastic strains on the specimen sides (cracks and damage to the specimen) decreased markedly, and the strain distribution and concentrated cracks (on the specimen sides) spread along the specimen in a monotonous manner (particularly in the area of ECC layers). It results in a significant decrease in the plastic strain, cracks, and damage intensity of the non-reinforced masonry specimen strengthened with ECC layers (especially with a two-sided cover on the entire bottom and top surface of the specimen) during the impact loading.

In addition, it is also demonstrated that in the reinforcement of non-reinforced masonry specimens with one ECC layer on the entire bottom surface and two ECC layers on the middle of the top surface (like one ECC layer on the entire bottom surface and one ECC layer on the sides of the top surface of the sample), ECC layers demonstrate poorer performance (and similar to that of the one-sided cover on the entire bottom surface of the sample) in the distribution of plastic strains along the specimen and finally shows a reduction in plastic strains, cracks, and damage intensities of the specimen during the impact loading.

Consequently, the obtained results generally demonstrate a proper performance of ECC reinforcement layers (especially on the whole top surface and sides of the lower surface of the specimen) concerning the uniform distribution of plastic strains along the non-reinforced masonry specimen during impact loading (reduction of plastic strains, cracks, and damage intensity of the specimen). By using ECC reinforcing layers on both sides of this specimen, the out-of-plane impact dynamic behavior of this specimen is improved significantly (compared to one-sided covering on the entire bottom surface of the sample, covering on the entire bottom and middle of the top surface of the sample, and covering on the whole bottom surface and sides of the top surface of the sample).

Figures 4a and b show that besides the reduction of the vertical impact displacement in the middle of the non-reinforced masonry specimen after reinforcing these specimens with ECC layers, this appropriate performance is improved with increasing ECC layers thickness, and ultimately, the improvement of the out-of-plane impact dynamic behavior of the non-reinforced masonry specimen retrofitted with ECC layers becomes more significant. The reason is that increasing ECC reinforcing layers thickness of the non-reinforced masonry leads to more increases in stiffness and out-of-plane strength of this specimen during the impact loading.

Therefore, an appropriate performance of ECC reinforcing layers is showed in the deformations reduction of the non-reinforced masonry specimens during the impact loading and finally enhanced the out-of-plane impact dynamic behavior of this specimen. By increasing the thickness of ECC layers, this behavior becomes more significant.

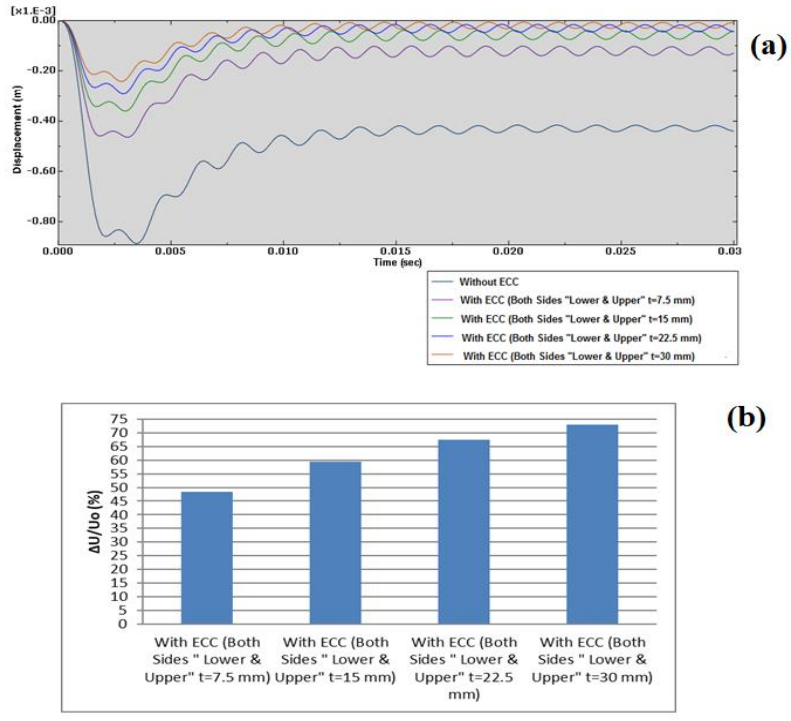

Fig. 4. Effect of ECC reinforcing layers and their thickness (with full connection) on the a) vertical displacement and b) on the reduction percentage of the vertical displacement in

the middle of the non-reinforced masonry specimen during vertical impact loading (E_ecc=17.5 GPA)

Figs. 5(a,b) show that retrofitting the non-reinforced masonry specimen with ECC layers (especially thicker ECC layers) increases the energy absorption of this specimen during the impact loading significantly, which results in more noteworthy energy dissipation (energy reduction) of the non-reinforced masonry sample retrofitted with ECC layers (especially thicker ECC layers) during the impact loading. Also, it is seen that after retrofitting the non-reinforced masonry specimen with thicker ECC layers, the placement of these layers on the top and bottom surface of the sample has more considerable performance in energy absorption and dissipation (energy reduction) of this sample during the impact loading. Using ECC reinforcing layers and increasing ECC layers thickness finally improve the out-of-plane dynamic behavior of this sample.

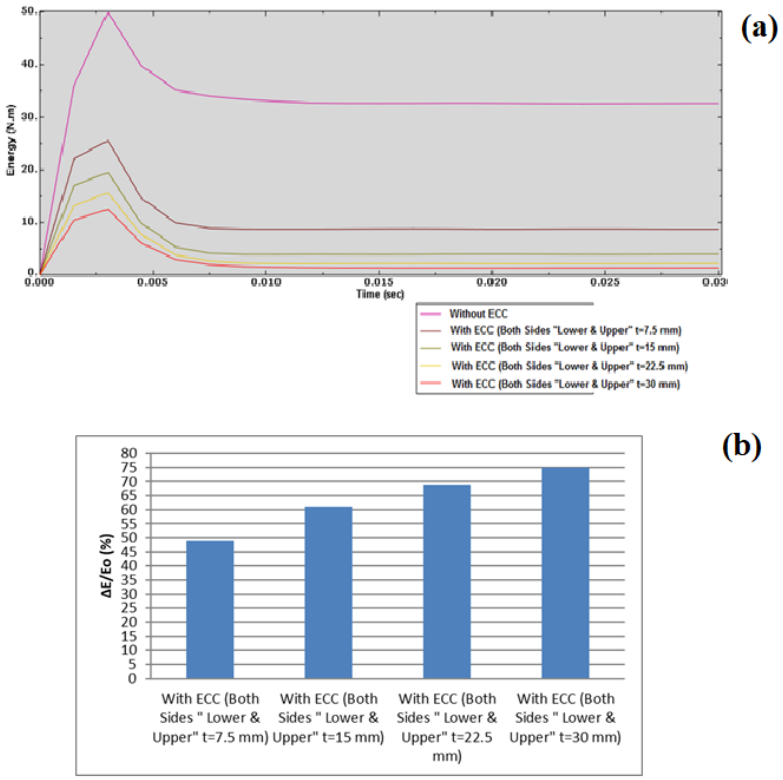

Fig. 5. Effect of ECC reinforcing layers and their thickness (with full connection) on the a) energy and b) energy reduction percentage of non-reinforced masonry specimen during the vertical impact loading (E_ecc=17.5 GPA)

Figures S9 and S10 illustrate that after retrofitting the non-reinforced masonry specimen with ECC layers (especially thicker ECC layers), the concentration of plastic strains distribution on the sides of the sample during the impact loading is significantly decreased, and these distributions and concentrated cracks (on the specimen sides) are spread with a uniform process along the specimen (especially in the ECC layers areas). This reduces the plastic strains, cracks, and damage to non-reinforced masonry specimens retrofitted with ECC layers (especially thicker ECC layers) during the impact loading. It can also be seen that, retrofitting the non-reinforced masonry specimen with thicker ECC layers results that the placement of these layers on both top and bottom surfaces of the specimen leads to more significant performance in uniform distribution of plastic strains along the specimen, and subsequently reduces the plastic strains, cracks, and damage intensity of the specimen during impact loading. Furthermore, the appropriate performance of ECC reinforcing layers in uniform distribution of plastic strains along the

non-reinforced masonry specimen under the impact loading improves the out-of-plane impact dynamic behavior of this specimen.

Figs 6a and 6b indicate that proper performance of ECC layers and improvement of out-of-plane impact dynamic behavior of the non-reinforced masonry sample retrofitted with ECC layers is more significant after reinforcement of this non-reinforced masonry specimen with ECC layers and by increasing the stiffness of the ECC layers. The reason is that increasing the elasticity modulus (stiffness) of ECC reinforcing layers causes more increase in the stiffness value and, ultimately, the out-of-plane strength of this sample during the impact loading. The figures generally confirm an appropriate performance of ECC reinforcing layers in reducing displacements of the non-reinforced masonry specimen during the impact loading and improvement of the out-of-plane dynamic behavior of this specimen, which is mainly due to the increasing ECC layers stiffness.

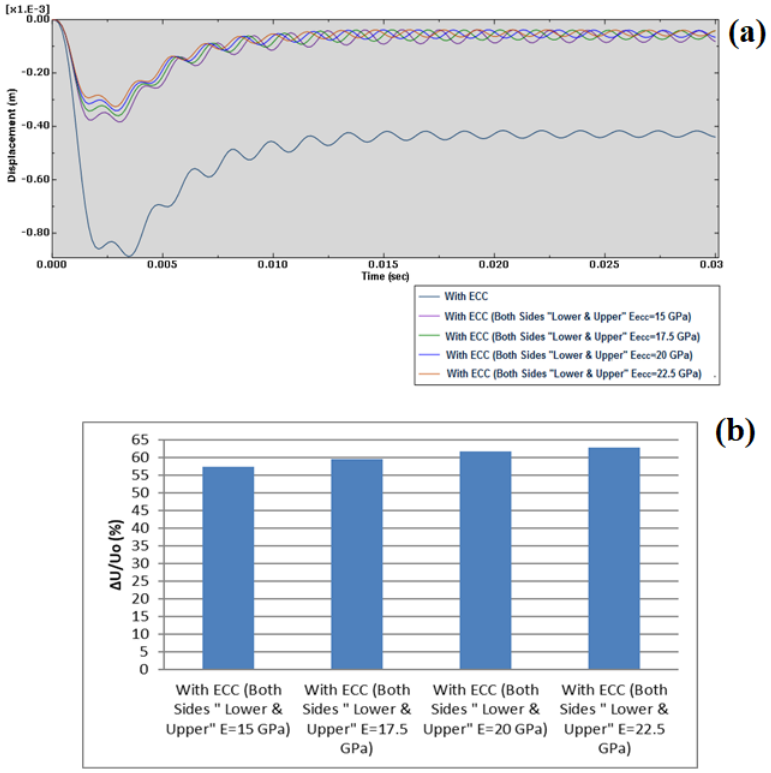

Fig. 6. Effect of ECC reinforcing layers and their stiffness (with full connection) on the a) vertical displacement and b) reduction percentage of the vertical displacement in the middle of the non-reinforced masonry specimen during the vertical impact loading (t= 15mm)

As can be shown from Figs. 7a and 7b, retrofitting the non-reinforced masonry specimen with ECC layers (especially ECC layers with more stiffness) increases significantly the energy absorption of this sample during the impact loading, resulting in significant energy dissipation (energy reduction). It can also be observed that after retrofitting the non-reinforced specimen with ECC layers having more stiffness, the placement of these layers on the top and bottom surfaces of the specimen has a significant impact on energy absorption and consequently, energy dissipation (energy reduction) of the sample. It is also concluded that the ECC layers stiffness improves the out-of-plane impact dynamic behavior during impact loading.

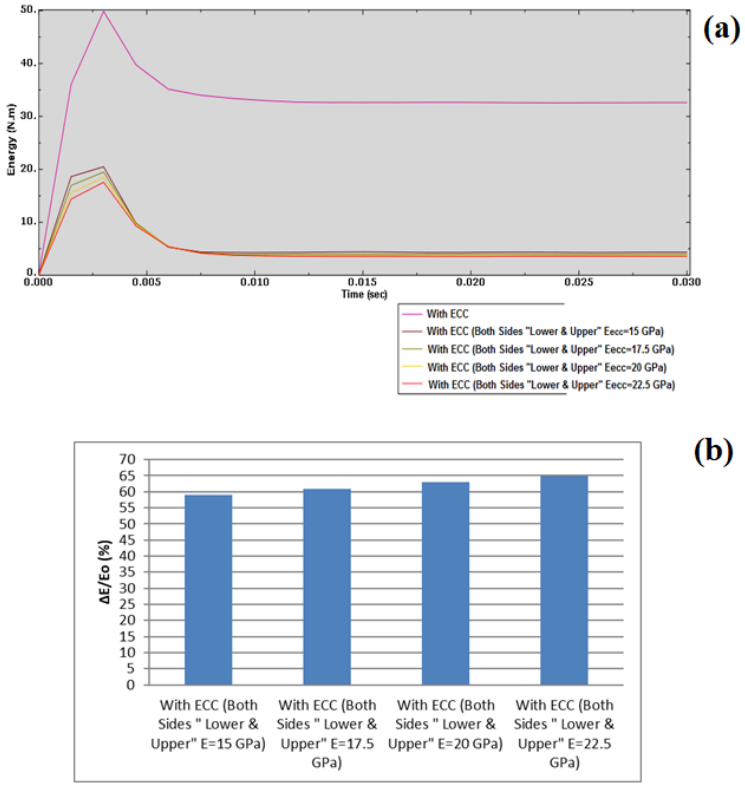

Fig. 7. Effect of ECC reinforcing layers and their stiffness (with full connection) on the a) energy and b) reduction percentage of the energy of the non-reinforced masonry specimen during the vertical impact loading (t=15mm)

As shown in figures S11 and S12, after retrofitting the non-reinforced masonry specimen with ECC layers (especially ECC layers having more stiffness), the concentration of plastic strain distribution on the sides of the specimen during the impact loading is decreased, and these concentrated strains and cracks (on sides of the specimen) are spread uniformly along the specimen (especially in the areas of ECC layers). It results in a significant reduction of the plastic strains, cracks, and damage intensity of the non-reinforced masonry retrofitted with ECC layers (especially ECC layers having more stiffness) during the impact loading. It is also demonstrated that after retrofitting the non-reinforced masonry with ECC layers with more stiffness, the placement of these layers on the top and bottom surfaces of the specimen has a greater impact on uniformly distributing plastic strains along the specimen and reducing plastic strain, cracks, and damage intensity of the specimen during the impact loading. Therefore, the improvement of the out-of-plane dynamic behavior of this specimen is enhanced by increasing the ECC layers' stiffness.

4. Conclusion

The following results were obtained:

1. The unreinforced masonry specimen with an ECC layer on the top surface had higher energy absorption and energy dissipation under the impact loading. Furthermore, the specimen with the ECC layer on top showed a more uniform distribution of plastic strains, lower plastic strains, cracks, and damage, and higher out-of-plane strength, with the vertical displacement in the middle declining under the impact loading.

2. The unreinforced masonry specimen with an ECC layer across the top surface and two ECC layers on the sides of the bottom surface had higher performance than the

specimen with an ECC layer on the top surface and an ECC layer in the middle of the bottom surface and showed similar performance to the specimen with double coverage across the top and bottom in terms of energy absorption and dissipation under impact loading. The specimen with an ECC layer on the top surface and an ECC layer in the middle of the bottom surface had lower performance (similar performance to the specimen with an ECC layer across the top surface) in energy absorption and dissipation under the impact loading.

3. The unreinforced masonry specimen with an ECC layer on the top surface and two ECC layers on the sides of the bottom surface outperformed the specimen with an ECC layer across the top surface and an ECC layer in the middle of the bottom surface in plastic strain uniformity, cracking, and damage reduction under impact loading. The unreinforced masonry specimen with an ECC layer across the top surface and an ECC layer in the middle of the bottom surface showed lower performance (similar to the specimen with a single-sided ECC layer on the top surface) in plastic strain uniformity along the specimen and plastic strain, cracking, and damage reduction under impact loading.

4. The unreinforced masonry specimen with an ECC layer across the top surface and two ECC layers in the middle of the top surface outperformed the specimen with an ECC layer across the bottom surface and an ECC layer on the sides of the top surface and showed similar performance to the specimen with ECC layers on both top and bottom in energy absorption and dissipation under impact loading. The specimen with an ECC layer across the bottom and an ECC layer on the sides of the top surface showed lower performance in plastic strain uniformity and plastic strain, cracking, and damage reduction under the impact load.

5. A rise in the ECC thickness further improved the performance of ECC layers in reducing the impact-induced vertical displacement in the middle of the unreinforced masonry specimen and enhanced dynamic out-of-plane behavior. Thicker ECC layers enhanced stiffness and out-of-plane strength under impact loading.

6. The use of thicker ECC layers on the top and bottom surfaces of the specimen led to even higher energy absorption and dissipation under the impact load. It also reduced plastic strains, cracks, and damage under impact loading.

7. Stiffener EC layers were more efficient and effective in diminishing the impact-induced vertical displacement in the middle of the unreinforced masonry specimen and improving dynamic out-of-plane behavior. An increased stiffness (elasticity modulus) of EEC layers would further increase the stiffness and out-of-plane strength of the unreinforced masonry specimen under impact loading.

8. The unreinforced masonry specimen strengthened with stiffener ECC layers on the top and bottom surfaces showed a higher performance in energy absorption and dissipation under impact loading. It also showed a more uniform distribution of plastic strains and lower plastic strains, cracks, and damage under impact loading.

Statements and Declarations: There is no conflict of interest.

Data Availability Statement: Data available on request from the authors.

References

Alimohammadi, V., Maghfouri, M., Nourmohammadi, D., Azarsa, P., Gupta, R., & Saberian, M. (2021). Stormwater runoff treatment using pervious concrete modified with various nanomaterials: A comprehensive review. Sustainability, 13(15), 8552, https://doi.org/10.3390/su13158552

Bernat-Maso, E., Escrig, C., Aranha, C. A., & Gil, L. (2014). Experimental assessment of Textile Reinforced Sprayed Mortar strengthening system for brickwork wallettes. Construction and Building Materials, 50, 226-236. https://doi.org/10.1016/j.conbuildmat.2013.09.031

Carozzi, F. G., Milani, G., & Poggi, C. (2014). Mechanical properties and numerical modeling of Fabric Reinforced Cementitious Matrix (FRCM) systems for strengthening of masonry structures. Composite structures, 107, 711-725, https://doi.org/10.1016/j.compstruct.2013.08.026

Dehghani, A., Nateghi-Alahi, F., & Fischer, G. (2015). Engineered cementitious composites for strengthening masonry infilled reinforced concrete frames. Engineering Structures, 105, 197-208, https://doi.org/10.1016/j.engstruct.2015.10.013

Deng, M., Dong, Z., & Ma, P. (2019). Cyclic loading tests of flexural-failure dominant URM walls strengthened with engineered cementitious composite. Engineering Structures, 194, 173-182, https://doi.org/10.1016/j.engstruct.2019.05.073

Deng, M., & Yang, S. (2018). Cyclic testing of unreinforced masonry walls retrofitted with engineered cementitious composites. Construction and Building Materials, 177, 395-408, https://doi.org/10.1016/j.conbuildmat.2018.05.132

Deng, M., & Yang, S. (2020). Experimental and numerical evaluation of confined masonry walls retrofitted with engineered cementitious composites. Engineering Structures, 207, 110249, https://doi.org/10.1016/j.engstruct.2020.110249

Dizhur, D., Ingham, J., Moon, L., Griffith, M., Schultz, A., Senaldi, I., . . . Centeno, J. (2011). Performance of masonry buildings and churches in the 22 February 2011 Christchurch earthquake. Bulletin of the New Zealand Society for Earthquake Engineering, 44(4), 279-296, https://doi.org/10.5459/bnzsee.44.4.279-296

Engineers, A. S. o. C. (2017). Seismic evaluation and retrofit of existing buildings.

Ghiassi, B., Soltani, M., & Tasnimi, A. A. (2012). Seismic evaluation of masonry structures strengthened with reinforced concrete layers. Journal of Structural Engineering, 138(6), 729-743., https://doi.org/10.1061/(ASCE)ST.1943-541X.0000513

Han, T.-S., Feenstra, P. H., & Billington, S. L. (2003). Simulation of highly ductile fiber-reinforced cement-based composite components under cyclic loading. Structural Journal, 100(6), 749-757.

Ismail, N., El-Maaddawy, T., & Khattak, N. (2018). Quasi-static in-plane testing of FRCM strengthened non-ductile reinforced concrete frames with masonry infills. Construction and Building Materials, 186, 1286-1298, https://doi.org/10.1016/j.conbuildmat.2018.07.230

Kadam, S. B., Singh, Y., & Li, B. (2014). Strengthening of unreinforced masonry using welded wire mesh and micro-concrete–Behaviour under in-plane action. Construction and Building Materials, 54, 247-257, https://doi.org/10.1016/j.conbuildmat.2013.12.033

Konthesingha, K., Masia, M. J., Petersen, R. B., Mojsilovic, N., Simundic, G., & Page, A. W. (2013). Static cyclic in-plane shear response of damaged masonry walls retrofitted with NSM FRP strips–An experimental evaluation. Engineering Structures, 50, 126-136, https://doi.org/10.1016/j.engstruct.2012.10.026

Kumar, S., & Rai, D. C. (2022). Enhancing Flexural Strength of Unreinforced Masonry Members Using Cementitious Matrix-Based Composites. In Stability and Failure of High Performance Composite Structures (pp. 125-142): Springer, https://doi.org/10.1007/978-981-19-2424-8_6

Leblouba, M., Altoubat, S., Karzad, A., Maalej, M., Barakat, S., & Metawa, A. (2022). Impact response and endurance of unreinforced masonry walls strengthened with cement-based composites. Paper presented at the Structures In Structures (Vol. 36, pp. 262-279), https://doi.org/10.1016/j.istruc.2021.12.028

Li, V. C., & Leung, C. K. (1992). Steady-state and multiple cracking of short random fiber composites. Journal of engineering mechanics, 118(11), 2246-2264, https://doi.org/10.1061/(ASCE)0733-9399(1992)118:11(2246)

Li, V. C., Mishra, D. K., Naaman, A. E., Wight, J. K., LaFave, J. M., Wu, H.-C., & Inada, Y. (1994). On the shear behavior of engineered cementitious composites. Advanced Cement Based Materials, 1(3), 142-149, https://doi.org/10.1016/1065-7355(94)90045-0

Luccioni, B., & Rougier, V. C. (2011). In-plane retrofitting of masonry panels with fibre reinforced composite materials. Construction and Building Materials, 25(4), 1772-1788, https://doi.org/10.1016/j.conbuildmat.2010.11.088

Maghfouri, M., Alimohammadi, V., Gupta, R., Saberian, M., Azarsa, P., Hashemi, M., . . . Roychand, R. (2022). Drying shrinkage properties of expanded polystyrene (EPS) lightweight aggregate concrete: A review. Case Studies in Construction Materials, e00919, https://doi.org/10.1016/j.cscm.2022.e00919

Maghfouri, M., Shafigh, P., Alimohammadi, V., Doroudi, Y., & Aslam, M. (2020). Appropriate drying shrinkage prediction models for lightweight concrete containing coarse agro-waste aggregate. Journal of Building Engineering, 29, 101148, https://doi.org/10.1016/j.jobe.2019.101148

Nezhad, R. S., Kabir, M. Z., & Banazadeh, M. (2016). Shaking table test of fibre reinforced masonry walls under out-of-plane loading. Construction and Building Materials, 120, 89-103, https://doi.org/10.1016/j.conbuildmat.2016.05.097

Niasar, A. N., Alaee, F. J., & Zamani, S. M. (2020). Experimental investigation on the performance of unreinforced masonry wall, retrofitted using engineered cementitious composites. Construction and Building Materials, 239, 117788, https://doi.org/10.1016/j.conbuildmat.2019.117788

Pan, Z., Wu, C., Liu, J., Wang, W., & Liu, J. (2015). Study on mechanical properties of cost-effective polyvinyl alcohol engineered cementitious composites (PVA-ECC). Construction and Building Materials, 78, 397-404, https://doi.org/10.1016/j.conbuildmat.2014.12.071

Renuka, S., & Mervin Sanjith, I. (2022). Strengthening of Damaged Masonry Walls Using Engineered Cementitious Composites: Experimental and Numerical Analysis. Advances in Civil Engineering, 2022, https://doi.org/10.1155/2022/6343179

Rezaei, M., Hamidi, A., & Farshi Homayoun Rooz, A. (2016). Investigation of peak particle velocity variations during impact pile driving process. Civil Engineering Infrastructures Journal, 49(1), 59-69, 10.7508/CEIJ.2016.01.005

Riahi, Z., Elwood, K. J., & Alcocer, S. M. (2009). Backbone model for confined masonry walls for performance-based seismic design. Journal of Structural Engineering, 135(6), 644-654, https://doi.org/10.1061/(ASCE)ST.1943-541X.0000012

Santa-Maria, H., & Alcaino, P. (2011). Repair of in-plane shear damaged masonry walls with external FRP. Construction and Building Materials, 25(3), 1172-1180, https://doi.org/10.1016/j.conbuildmat.2010.09.030

Sharbatdar, M. K., & Tajari, A. (2021). Experimental in-plane seismic strengthening of masonry infilled reinforced concrete frames by engineered cementitious composites (ECC). Construction and Building Materials, 293, 123529, https://doi.org/10.1016/j.conbuildmat.2021.123529

Singh, S., Patil, R., & Munjal, P. (2017). Study of flexural response of engineered cementitious composite faced masonry structures. Engineering Structures, 150, 786-802, https://doi.org/10.1016/j.engstruct.2017.07.089

Soleimani-Dashtaki, S., Ventura, C. E., & Banthia, N. (2017). Seismic strengthening of unreinforced masonry walls using sprayable eco-friendly ductile cementitious composite (EDCC). Procedia engineering, 210, 154-164, https://doi.org/10.1016/j.proeng.2017.11.061

Tabrizikahou, A., Kuczma, M., Łasecka-Plura, M., & Noroozinejad Farsangi, E. (2022). Cyclic behavior of masonry shear walls retrofitted with engineered cementitious composite and pseudoelastic shape memory alloy. Sensors, 22(2), 511, https://doi.org/10.3390/s22020511

van Zijl, G. P. (2007). Improved mechanical performance: Shear behaviour of strain-hardening cement-based composites (SHCC). Cement and Concrete Research, 37(8), 1241-1247, https://doi.org/10.1016/j.cemconres.2007.04.009

Yardim, Y., & Lalaj, O. (2016). Shear strengthening of unreinforced masonry wall with different fiber reinforced mortar jacketing. Construction and Building Materials, 102, 149-154, https://doi.org/10.1016/j.conbuildmat.2015.10.095

Zamani Ahari, G., & Yamaguchi, K. (2021). Experimental study of in-plane hysteretic behavior of unreinforced masonry walls retrofitted with engineered cementitious composites (ECC). European Journal of Environmental and Civil Engineering, 1-20, https://doi.org/10.1080/19648189.2021.2023652 https://doi.org/10.1080/19648189.2021.2023652

Zhang, J., Maalej, M., & Quek, S. (2004). Hybrid fiber Engineered Cementitious Composites (ECC) for impact and blast-resistant structures. Paper presented at the Proceedings of the First International Conference on Innovative Materials and Technologies for Construction and Restoration–IMTCR04.

Supplementary Materials

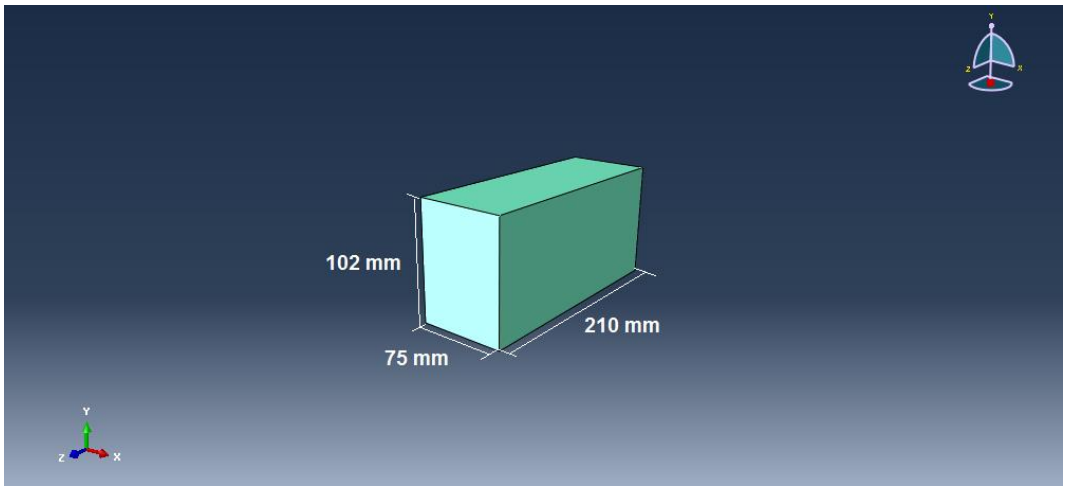

Fig. S1. Geometry model of equivalent blocks

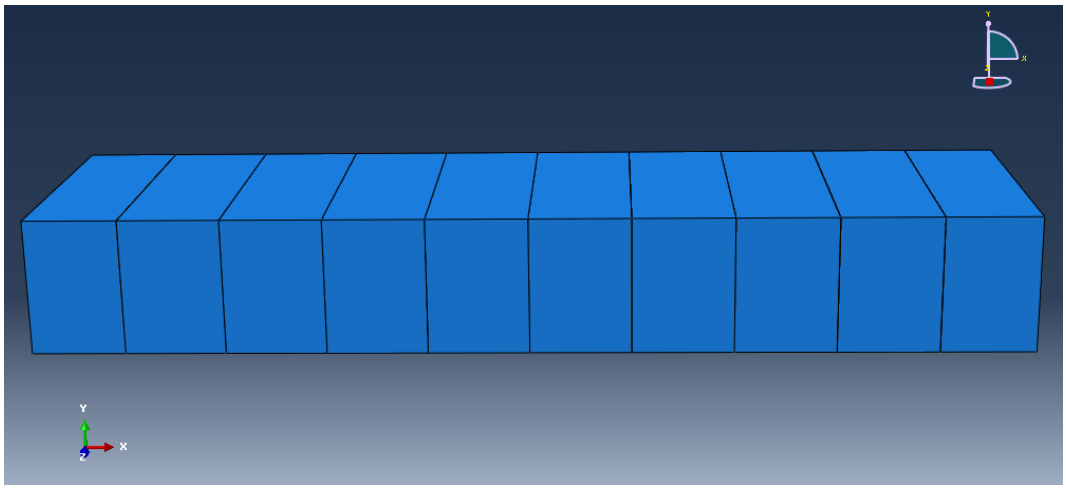

Fig. S2. Geometry layouts of equivalent blocks in models

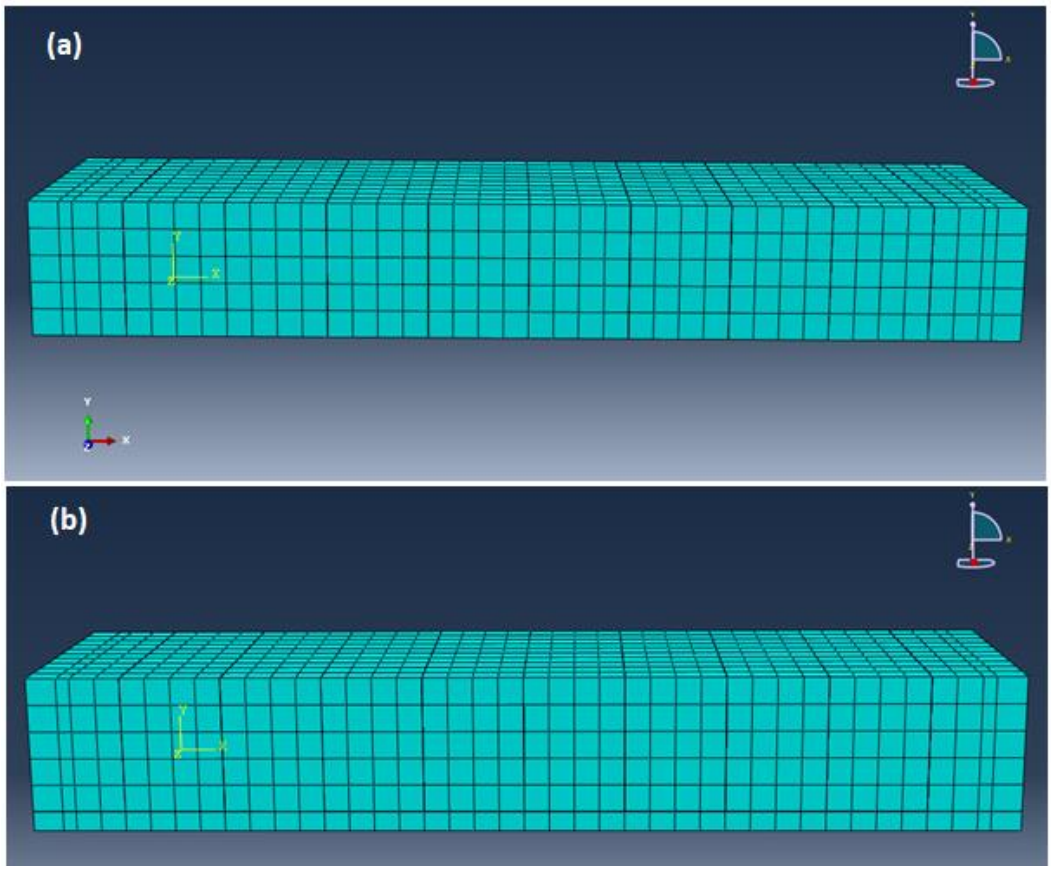

Fig. S3. Meshing geometric models of a) the non-reinforced non-retrofitted masonry sample b) the non-reinforced retrofitted masonry sample with one layer of ECC in the whole bottom surface of the sample

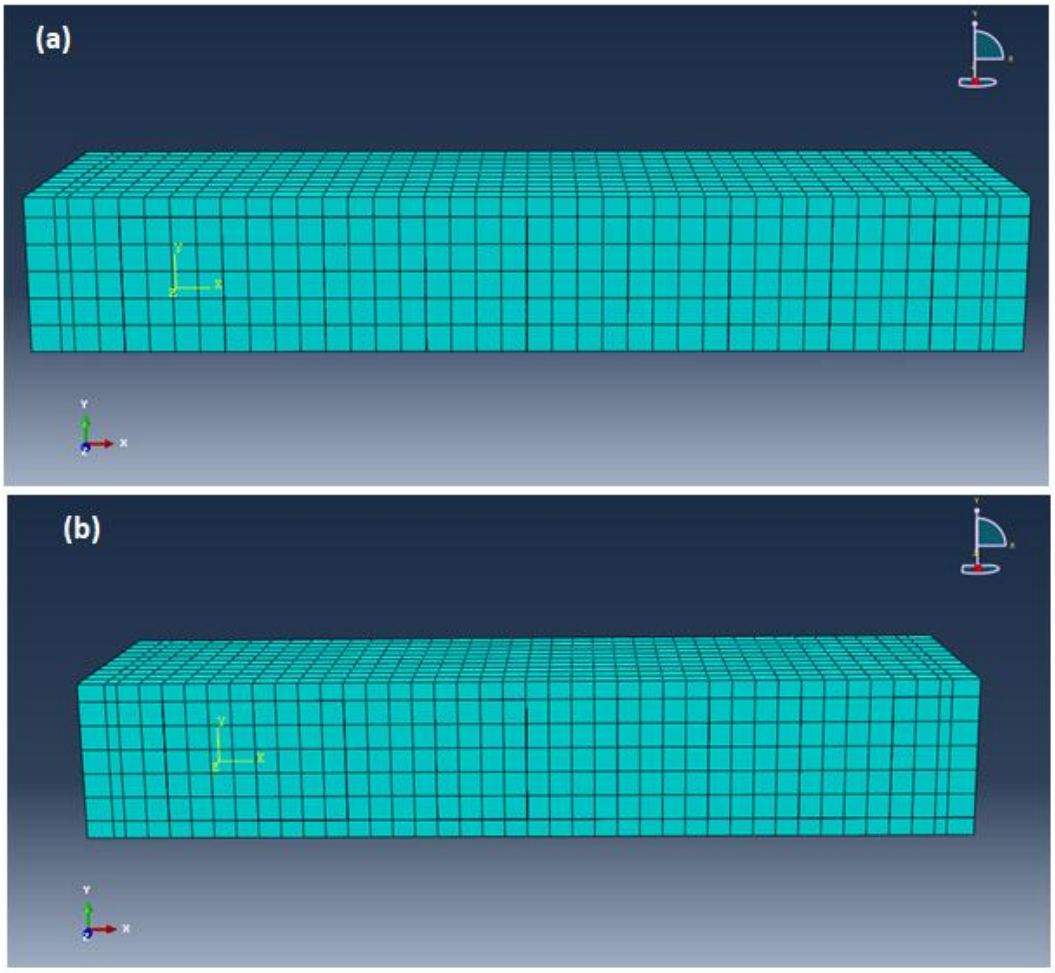

Fig. S4. Meshing geometric models of the non-reinforced retrofitted masonry sample with a) one layer of ECC in the whole top surface of the sample b) two layers of ECC in the whole bottom and top surfaces of the sample

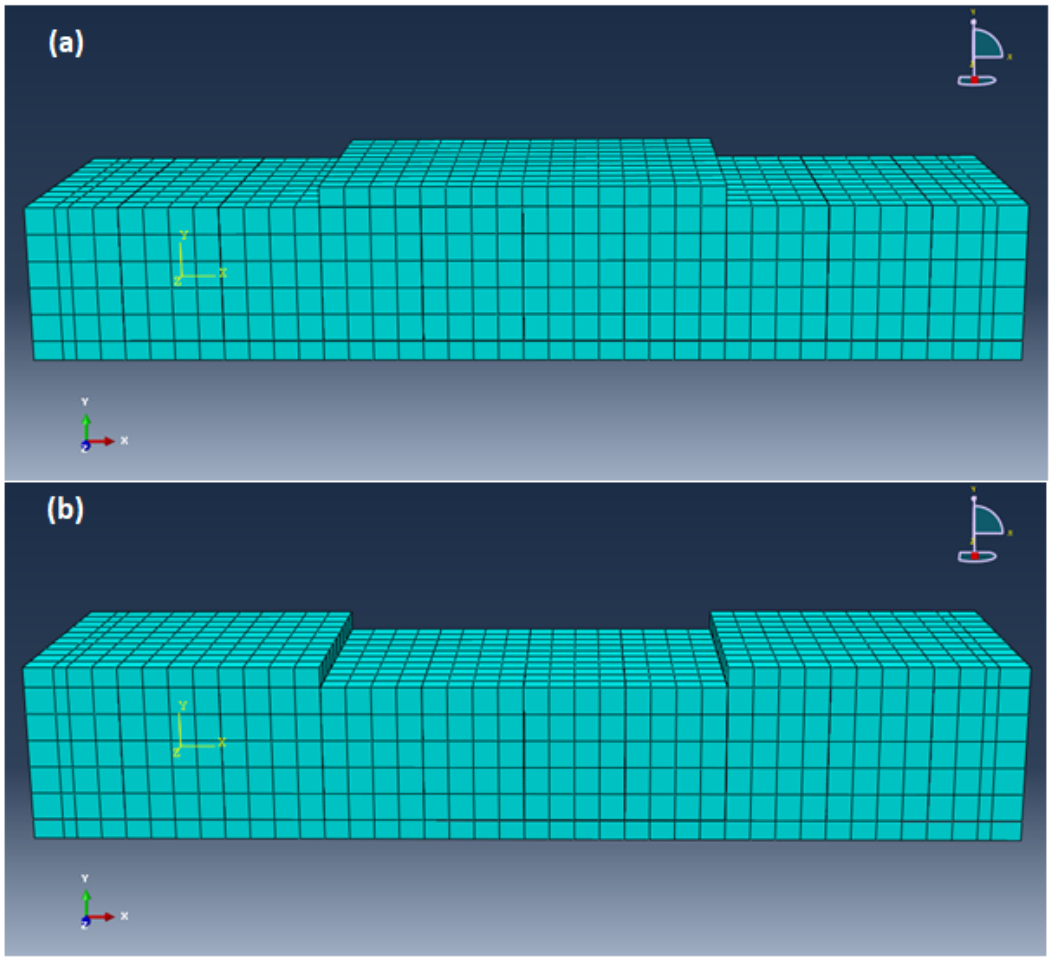

Fig. S5. Meshing geometric models of the non-reinforced retrofitted masonry sample with one layer of ECC in the whole of the sample at a) bottom and top surfaces b) bottom surface and two layers of ECC in lateral areas of the top surface

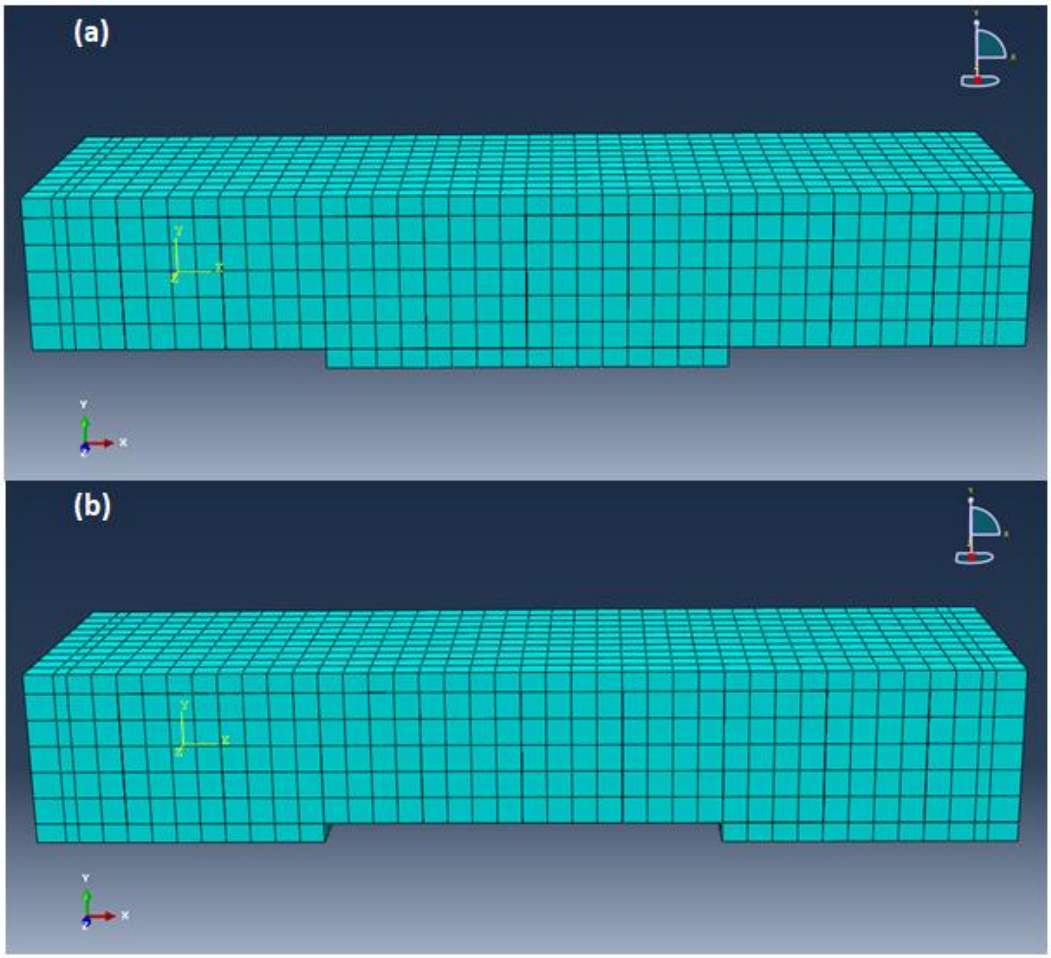

Fig. S6. Meshing geometric models of the non-reinforced retrofitted masonry sample with one layer of ECC in the whole top surface of the sample at a) one layer of ECC in the middle of the sample (bottom surface), and b) two layers of ECC in lateral areas of the sample (bottom surface)

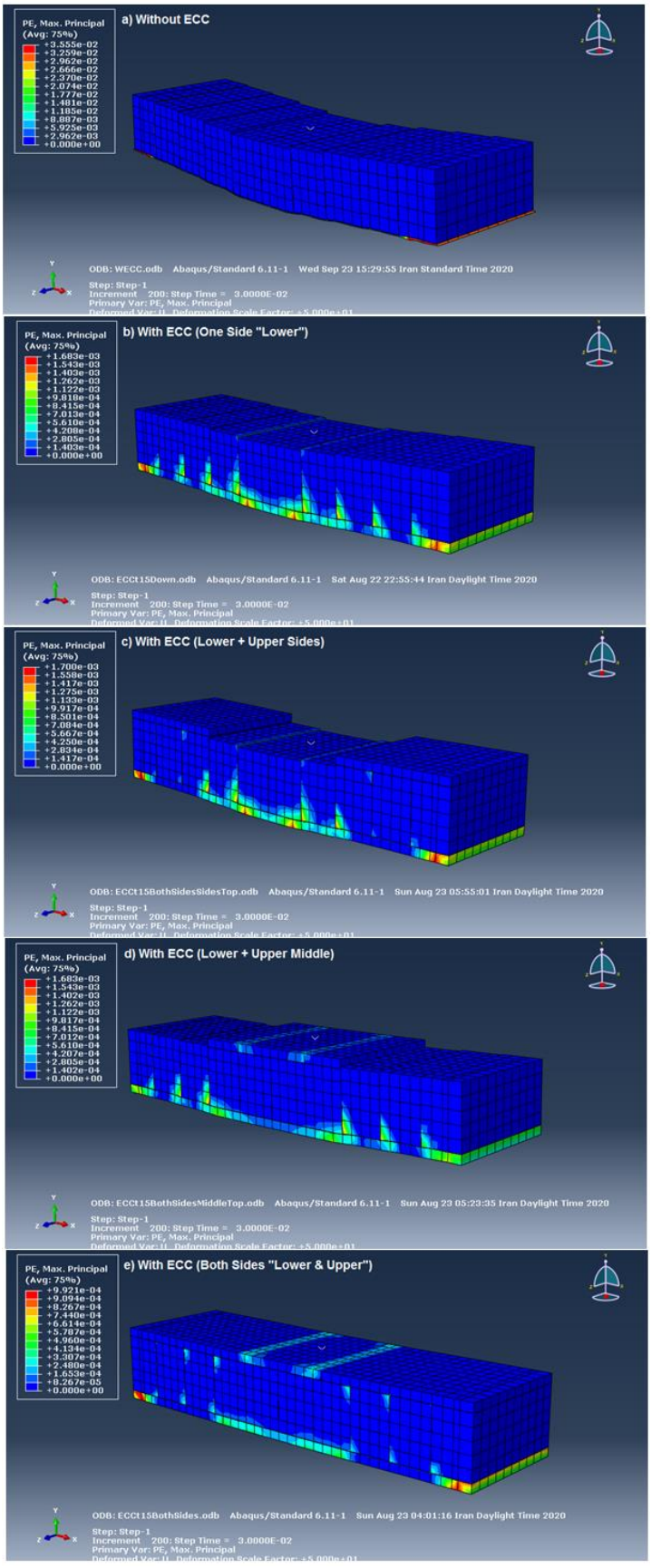

Fig. S7. Effect of ECC reinforcing layers and the top layer placement location (middle or sides of the top surface with full connection) on the intensity and process of the plastic strain distribution

of non-reinforced masonry during vertical impact loading in two-sided cover (t=15 mm، E_ecc=17.5 GPA)

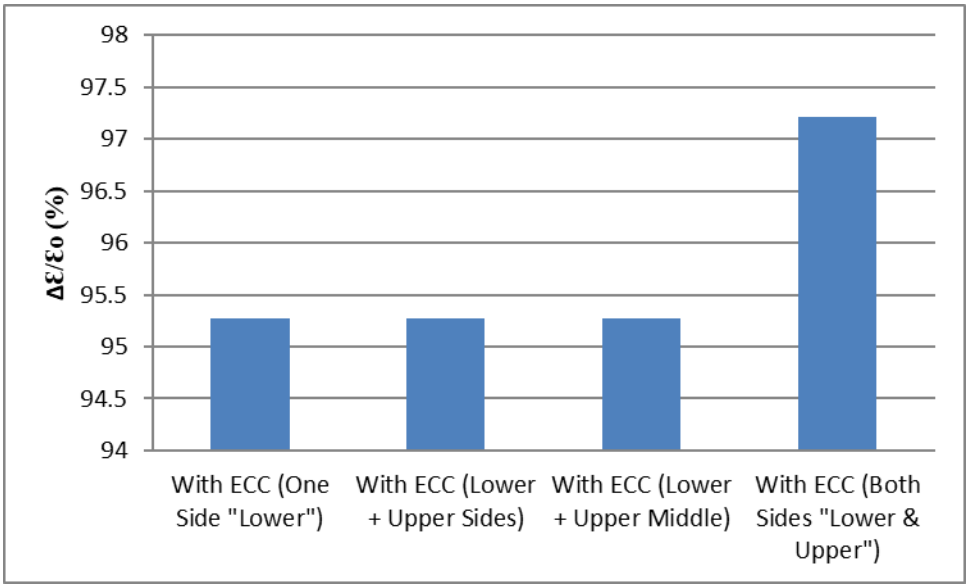

Fig. S8. Effect of top layer placement location (middle or sides of the top surface with full connection) on the reduction percentage of plastic strains of non-reinforced masonry during vertical impact loading in two-sided cover (t=15 mm، E_ecc=17.5 GPA)

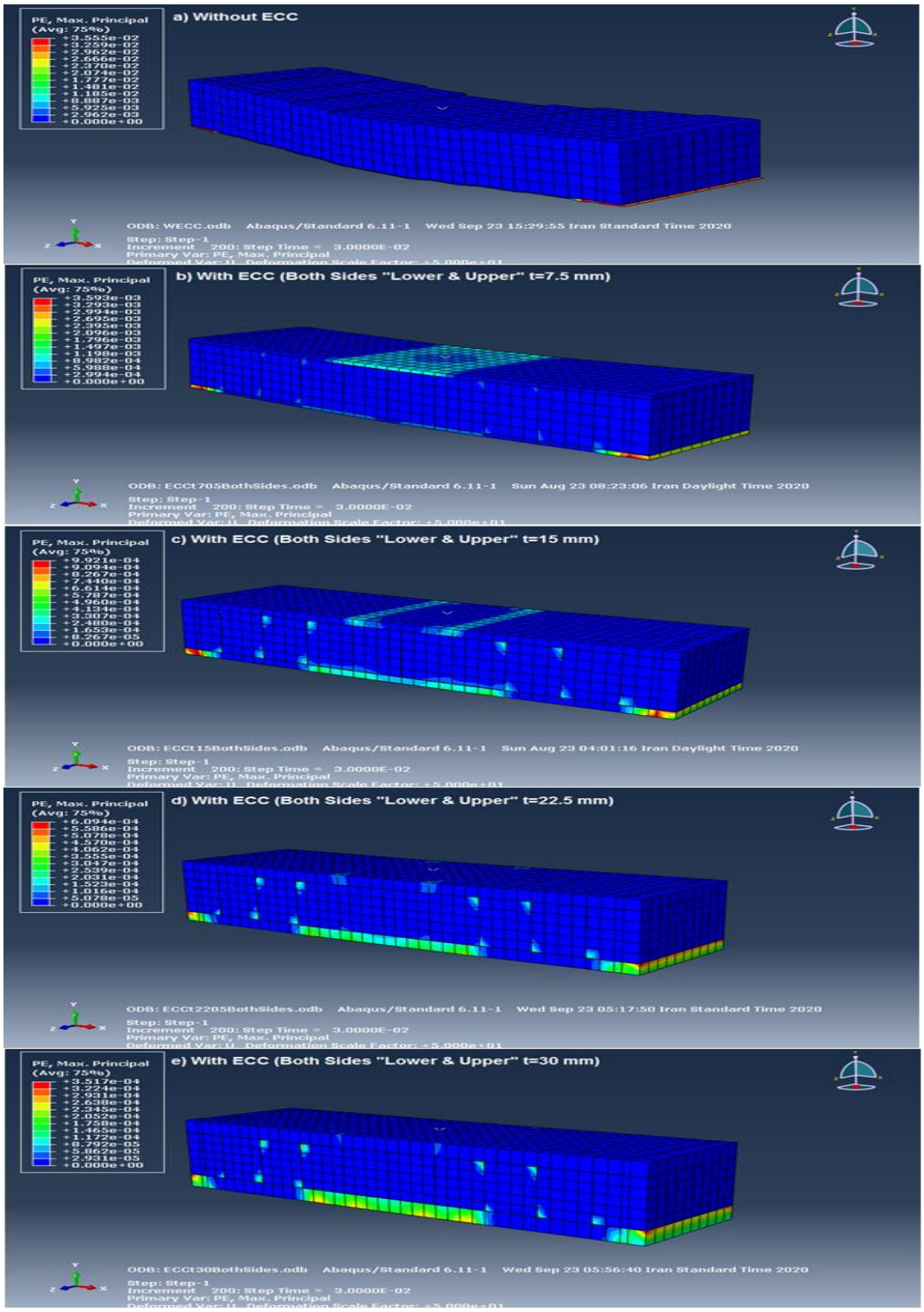

Fig. S9. Effect of ECC reinforcing layers and their thickness (with full connection) on the intensity and process of plastic strains distribution of non-reinforced masonry specimen under vertical impact loading (E_ecc=17.5 GPA)

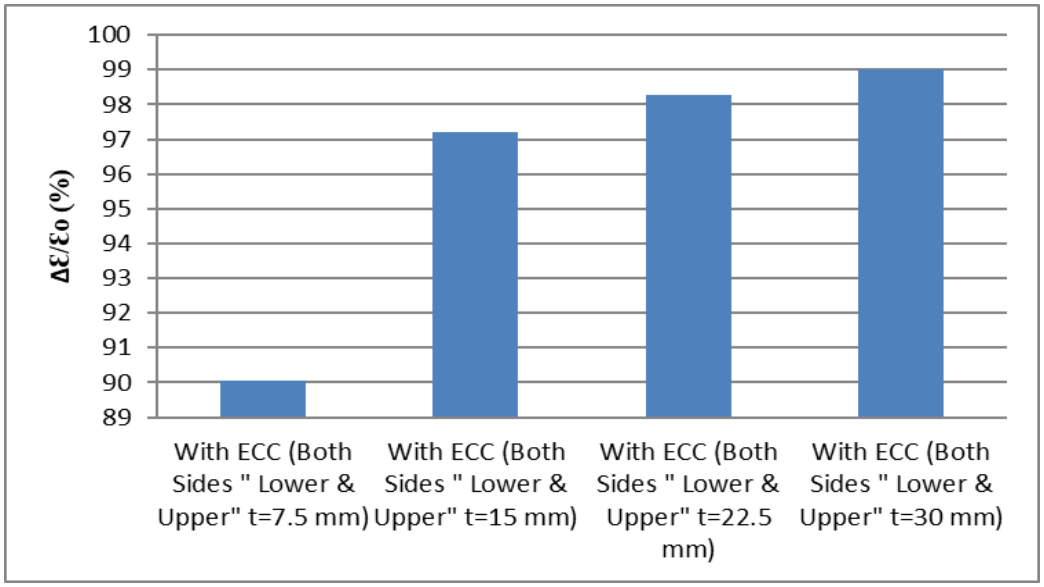

Fig. S10. Effect of ECC reinforcing layers thickness (with full connection) on the reduction percentage of plastic strains of the non-reinforced masonry specimen under vertical impact loading (E_ecc=17.5 GPA)

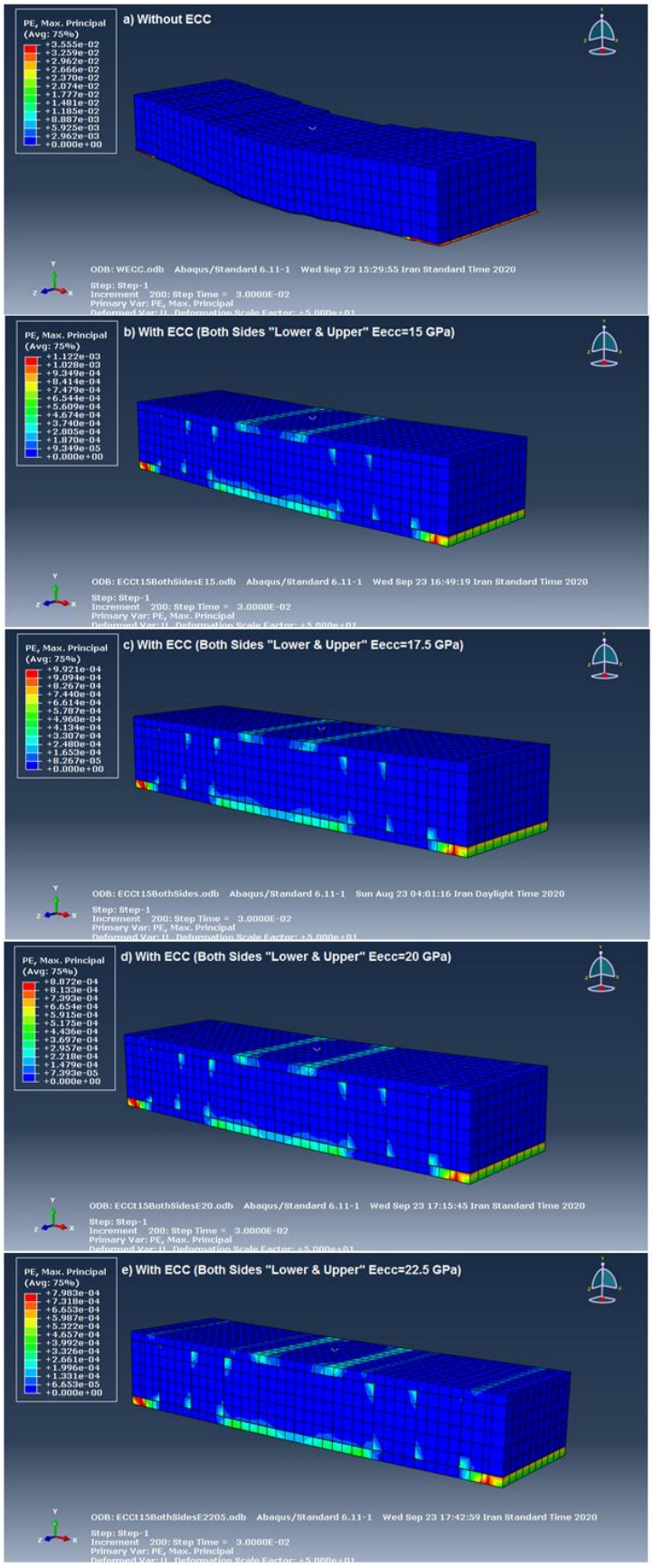

Fig. S11. Effect of ECC reinforcing layers and their stiffness (with full connection) on the intensity and process of the plastic strain distribution of the non-reinforced masonry specimen during the vertical impact loading (t=15 mm)

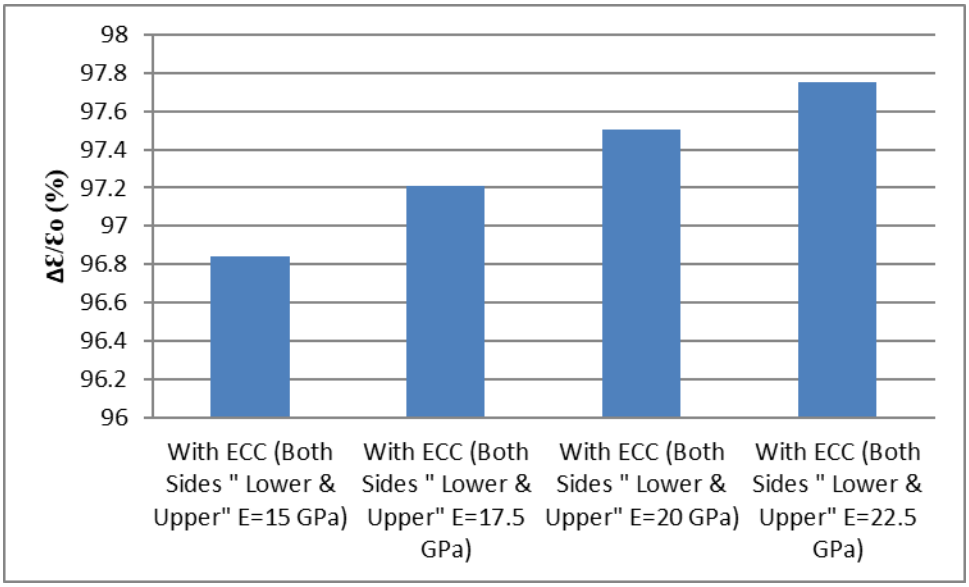

Fig. S12. Effect of ECC reinforcing layers stiffness (with full connection) on the reduction percentage of the intensity of the plastic strain distribution of the non-reinforced masonry specimen during the vertical impact loading (t=15 mm)

Table S1. The maximum lateral load-bearing of the laboratory sample during the experiment (Papanicolaou, Triantafillou et al. 2011) and numerical analysis

Max. Lateral Bearing (KN) (Experimental)	**Max. Lateral Bearing (KN) (Numerical)**	**Tolerance (%)**
6.35	6.75	6.3